Asian Pub. Corp.

www.asianpubs.org

ARTICLE

Molecular Docking Studies of Some Natural Products Against SARS-CoV-2 Main Protease: Potential Therapeutic Agents for COVID-19

Gnanavel Sadhasivam✉

ABSTRACT

The severe form of respiratory disease (COVID-19), caused by SARS-COV-2 virus, has evolved into a pandemic is the defining global health crisis of our time and greatest challenge we have faced since second World War. Hence, the current situation demands an immediate need to explore all the possible therapeutic strategies that can be control spread of the diseases. We identified potent COVID-19 M^{pro} inhibitors based on molecular docking studies on 24 known antiviral natural compounds, which are from medicinal plants and marine sponges. The results revealed that 15 potential COVID-19 main protease inhibitors have been identified among the 24 natural compounds of plants and marine origin. The result further revealed that the selected natural products that has lower free binding energy is Halituline (-8.41 Kcal/mol). As these active compounds were extensively validated by molecular docking, the chance that at least few of these compounds could be bioactive is excellent.

KEYWORDS

COVID-19, SARS-CoV-2, Docking, Binding energy, Natural product.

Asian Journal of Organic & Medicinal Chemistry

Volume: 5 Year: 2020
Issue: 3 Month: July–September
pp: 254–264
DOI: https://doi.org/10.14233/ajomc.2020.AJOMC-P288

Received: 12 August 2020
Accepted: 11 September 2020
Published: 15 September 2020

Author affiliations:

Research and Project Centre for Chemical and Biological Science, CHEMKOVIL, Mettur Dam, Salem-636402, India

✉To whom correspondence to be addressed:

E-mail: gnanamphd@gmail.com

Available online at: http://ajomc.asianpubs.org

INTRODUCTION

Coronavirus is an enveloped, positive sense single standard RNA virus belonging to coranaviridae family. The severe acute respiratory syndrome (SARS) is a serious life-threatening upper respiratory tract disease with the most common symptoms of cough, higher fever, headache, rigor, myalgia and dizziness. In humans, it mainly causes common cold, but complication including pneumonia and SARS can occur [1]. In 2003, SARS abruptly emerged and spread widely. The known human coronavirus (HCoV) includes HCoV-229E, HCoV-OC43, HCoV-NL63, HCoV-HKU1 and the more widely known severe acute respiratory syndrome coronavirus (SARS-CoV) becoming an epidemic that seriously affected public, which caused a global threat with high mortality and the economy of many countries [2-4]. But SARS has been controlled and no known SARS transmission has been recorded anywhere in the world after 2004. However, In 2012, World Health Organization (WHO) designated a sixth type of HCoV infection identified as the Middle East Respiratory Syndrome coronavirus (MERS-CoV), the mutant characteristic of the coronavirus that is the causative agent of SARS indicated the possibility of a re-emergence, which is associate with high fatality [5].

SARS-CoV-2 is a novel virus responsible for an outbreak of respiratory illness known as COVID-19, which has spread to several countries around the world. Towards the year end of December 2019, a novel coronavirus (nCoV-2019) with human-to-human transmission and severe human infection, originating in Wuhan, China was known [6]. This virus has affected many peoples in China and extended to other countries in a short time. On January 30, 2020, the Director-General of World Health Organizations (WHO) declared that the outbreak of COVID-19 constitutes a public health emergency of international concern. According to the report of WHO, as on September 10, 27,738,179 cases, including 899,916 deaths, have been confirmed globally; 4,645,519 cases, including 224,145 deaths in European region, 14,337,245 cases, including 498,255 deaths in region of the Americas, 2,055,446 cases, including 54,064 deaths in Eastern Mediterranean region, 530,403 cases, including 11,506 deaths in Western Pacific region, 5,067,207 cases, including 88,418 deaths in South-East Asia region, 1,101,618 cases, including 23,515 death in African region have been reported [7]. This pandemic disease is still ongoing, so it is urgent to find novel preventive treatment and therapeutic agents as soon as possible.

While specific vaccines and antiviral agents are the most effective methods to prevent and treat viral infection, there are not yet effective treatments that target the COVID-19. Development of these treatments may require months or years, meaning that a more immediate treatment or control mechanism should be found if possible. Natural product used in traditional medicine present a potentially valuable resource to this end [8]. Therefore, great attention has been paid to the secondary metabolites secreted by medicinal plants in tropical regions that may be developed as medicines. Several compounds from medicinal plants (including marine sponge), such as alkaloid, limonoids, flavonoids, carbohydrates, glycosides, polyphenols and tannins have been reported to have antiviral bioactivities. In the present study, 24 compounds were investigated from medicinal plants, marine sponges and marine tunicate as potential inhibitor candidates for COVID-19 Main protease (PDB ID: 6YB7). The results of the present study will provide other researchers with opportunities to identify the right drug to fight COVID-19 Main protease (COVID-19 M^{pro}).

EXPERIMENTAL

Compounds selection: Google and PubMed literature concerning natural compounds against SARS or MERS cononavirus activity and HIV protease inhibitors were selected using the query "antiviral activity of protease inhibitors", natural product as antiviral compounds", "natural product for invade corona virus" and "antiviral marine compounds". After careful reading of the studies returned by this search, natural compounds 1,5-dicaffeoylquinic acid, 22-O-(N-Me-L-valyl)-21-epiafl-aquinolone B, arisugacin A, azadirachtin, baicalin, berberine, butulinic acid, calonolide, conocurvone, cryptotanshinone, didemnin, gomisin A, halitulin, hypoglaumine B, lithosperimic acid, lycorine,papaverine, papuamide A, repandusinic acid, sansalvamide A, sorbicatechol A, swertifrancheside and tanshinone II A that have been biologically reported for antiviral activities were selected.

Proteins/macromolecules: COVID-19 SARS-CoV-2 main protease (PDB ID: 6YB7) structure was obtained from PDB (https://www.rcsb.org/), in PDB format [9]. PDB is a library for the crystal structure of biological macromolecules, worldwide. Molecular docking of ligands onto the COVID-19 M^{pro} was carried out using the Auto-Dock tool (Version 4.2). Accelrys discovery studio client 4.1 visualizer was used for the visualizing protein-ligand complex. All bounded water, solvents and ligands were eliminated from the protein and polar hydrogens were added. The active site aminoacid residues are chosen as PHE140, LEU141, ASN142, CYS145, HIS163, ARG40 and ASN84.

Ligand preparation: The three-dimensional structures of all selected ligands were constructed using Chembio 3D ultra 13.0 software, and then they were energetically minimized using MMFF94. 3D structure of ligands was optimized using Gaussian 09W software using 6-31 G basis set before docking.

Molecular docking: The molecular docking studies were performed by the reported method [10]. Molecular docking of all energy minimized molecules was carried out with crystal structures of COVID-19 M^{pro} using the Auto-Dock tool. The crystal structure of the protein was taken from Protein Data Bank (https://www.rcsb.org/) and chain A was selected for docking studies. All bounded water and ligands were eliminated from the protein and polar hydrogen was added to the protein as it is required for the electrostatics and then nonpolar hydrogen atoms were merged together. The files were generated as PDBQT format with all the default values accepted. Moreover, all docking grid box size is 60 × 60 × 60 points in X, Y and Z direction. A grid spacing of 0.375 Å and 15 runs were generated using Lamarckian genetic algorithm searches. The docking parameters were used as default in Autodock tool.

Drug-like properties: Drug-like properties were calculated using Lipinski's rule of five, which proposes that molecules with poor permeation and oral absorption have molecular weights > 500, C Log P > 5, more than 5 hydrogen bond donors and more than 10 acceptor groups [11] Adherence with Lipinski's rule of five as calculated using molinspiration prediction (https://www.molinspiration.com/cgi-bin/properties).

RESULTS AND DISCUSSION

Since the outbreak of novel coronavirus disease COVID-19, caused by the SARS-CoV-2 infection, has evolved into a pandemic resulting in significant mortality. The COVID-19 virus belongs to family coronaviridae and which is an enveloped virus with a positive sense single-stranded RNA genome. Effective human to human transmission even by symptom or without symptom has been a major reason underlying the fast worldwide spread of disease [12]. More morbidity has been found among the elderly, those with additional comorbidities and those under less immunity power. Considering this potential threat of a pandemic COVID-19, scientists are racing to understand this new virus and discover effective therapeutic medicine. It is urgent to develop effective broad-spectrum virus replication inhibitors to handle patient with COVID-19. Blocking key proteases such as coronavirus main protease (3CL pro) and papain-like protease (PL^{pro}) are considered to be critical in blocking viral life cycles since they are essential for the proteolysis of

viral polyprotein into functional units. Recently many protease inhibitors for SARS-CoV-2 reported from medicinal plants and marine plants [13]. In present study, we investigated the inhibition of SARS-CoV-2 main protease (PDB :6YB7) by natural products derived from medicinal and marine plants. Natural compounds have been used since ancient times and are well accepted as sources of drugs in several human diseases. The healing ability of these natural compounds draw interest to study natural products as a potentially important resource of drug molecules, they are evolutionarily optimized as drug-like molecules and remain the better sources of drug and drug leads [14].

Pharmacokinetic properties: Drug like properties of all selected natural compounds to be considered as drug candidates were based on Lipinski's rule of five. This rule is formulated for mainly orally administered drugs, it uses four criteria to establish if a molecules is drug like; to have a molecular weight of 500 or less than 500, a logarithm of partition coefficient (C Log P) ≤ 5, hydrogen bond donor sites ≤ 5 and hydrogen bond acceptor site ≤ 10. Among the 24 selected natural compounds, 9 compounds well followed the rule of five (zero violation), 4 compounds showed 1 violation, 3 compounds showed 2 violation and 8 compounds showed 3 violation (Table-1). Though many selected compounds showed Lipinki's rule violations, natural products and drugs are exception to follow this rule [15] and the selected all molecules were subjected to molecular docking studies onto COVID-19 M^{pro} (Fig. 1).

Molecular docking studies: Molecular docking studies are used to find the binding affinity of ligand to specific target protein [16]. The natural products alkaloids, terpenoids,

TABLE-1
STRUCTURE AND DRUG-LIKE PROPERTIES OF SELECTED NATURAL COMPOUNDS USED IN DOCKING STUDIES ONTO COVID-19 M^{pro}

Structure, name and molecular formula of the selected compounds	Lipinski's properties	Source and antiviral	Ref.
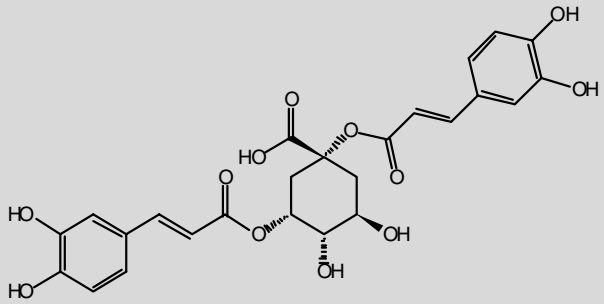 1,5-Dicaffeoylquinic acid ($C_{25}H_{24}O_{12}$)	m.w.: 516.4 HBD: 7 HBA: 12 C log P: -0.19 Violations: 3	*Cynara cardunculus* (Plant)	[17]
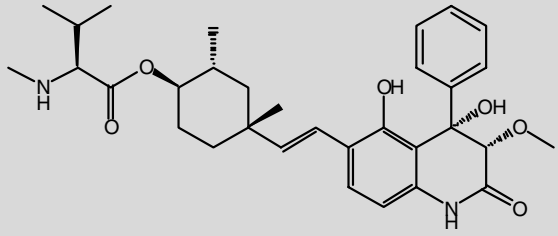 22-O-(N-Me-L-valyl)-21-epiaflaquinolone B ($C_{32}H_{42}N_2O_6$)	m.w.: 550.7 HBD: 4 HBA: 8 C log P: 4.7 Violations: 1	*Aspergillus sp. XS-20090B15* (Marine fungi)	[18]
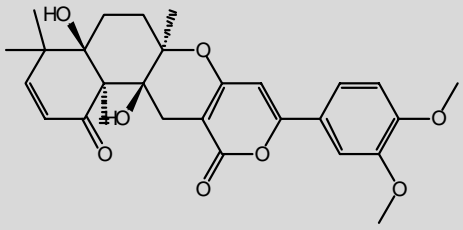 Arisugacin A, $C_{28}H_{32}O_8$	m.w.: 496.5 HBD: 8 HBA: 2 C log P: 3.5 Violations: 0	*Aspergillus terreus* SCSGAF0162 (Marine fungi)	[19]
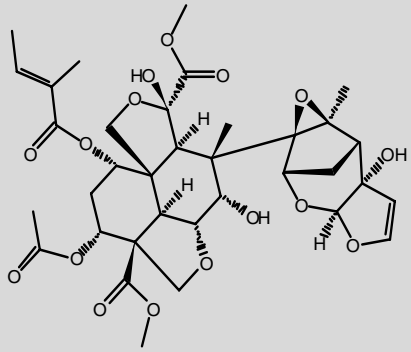 Azadirachtin ($C_{35}H_{44}O_{16}$)	m.w.: 720.7 HBD: 3 HBA: 16 C log P: -0.5 Violations: 2	*Azadirachta indica* (Neem seeds)	[20]

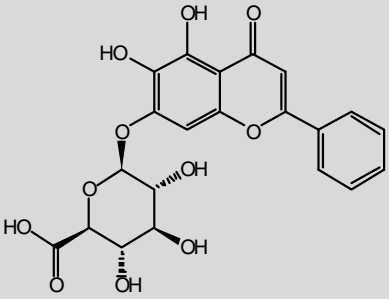

Baicalin ($C_{21}H_{18}O_{11}$)

m.w.: 446.3
HBD: 6
HBA: 11
C log P: 0.7
Violations: 2

Scutellaria baicalensis
(Plant)

[21]

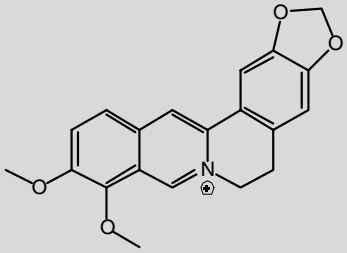

Berberine ($C_{20}H_{18}NO_4$)

m.w.: 336.3
HBD: 0
HBA: 5
C log P: -0.7
Violations: 0

Berberis aristata
(Plant)

[22]

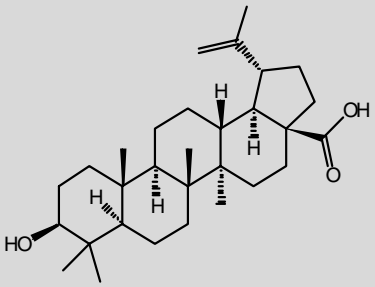

Butulinic acid ($C_{30}H_{48}O_3$)

m.w.: 456.7
HBD: 2
HBA: 3
C log P: 8.4
Violations: 1

Betula pubescens,
Prunella vulgaris
(Plant)

[23]

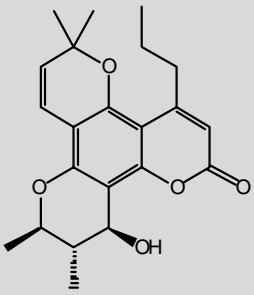

Calonolide A ($C_{22}H_{26}O_5$)

m.w.: 370.4
HBD: 1
HBA: 5
C log P: 4.7
Violations: 0

Calophyllum lanigerum
(Plant)

[24]

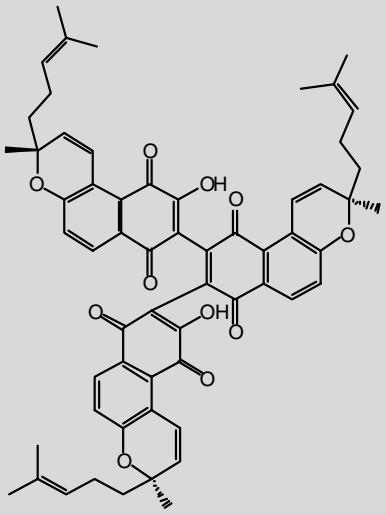

Conocurvone ($C_{60}H_{56}O_{11}$)

m.w.: 953.1
HBD: 2
HBA: 11
C log P: 15.3
Violations: 3

Conospermum incurvum
(Plant)

[25]

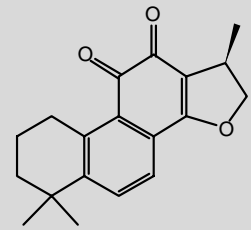 Cryptotanshinone ($C_{19}H_{20}O_3$)	m.w.: 296.1 HBD: 0 HBA: 3 C log P: 3.3 Violations: 0	*Salvia miltiorrhiza* (Plant)	[26]
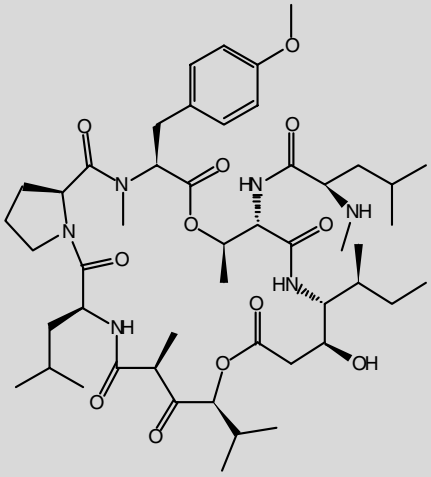 Didemnin A ($C_{49}H_{78}N_6O_{12}$)	m.w.: 943.19 HBD: 5 HBA: 18 C log P: 7.2 Violations: 3	*Didemnid tunicate* (Sea squirt)	[27]
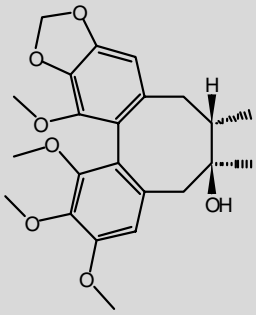 Gomisin A ($C_{23}H_{28}O_7$)	m.w.: 416.4 HBD: 1 HBA: 7 C log P: 3.9 Violations: 0	*Schisandra chinensis* (Plant)	[28]
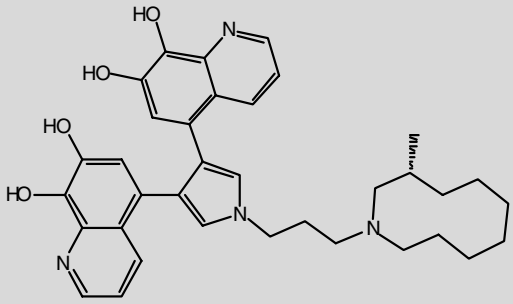 Halitulin ($C_{49}H_{78}N_6O_{12}$)	m.w.: 580.7 HBD: 4 HBA: 8 C log P: 8.6 Violations: 2	*Haliclona tulearensis* (Marine sponge)	[29,30]
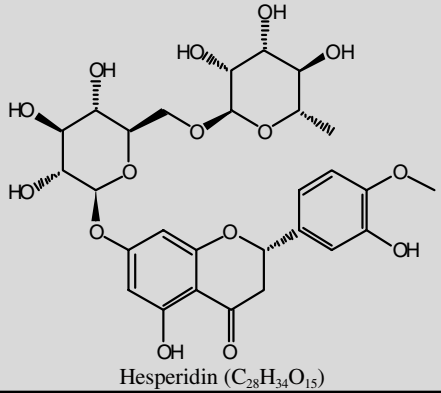 Hesperidin ($C_{28}H_{34}O_{15}$)	m.w.: 610.5 HBD: 8 HBA: 15 C log P: -0.2 Violations: 3	*Citrus sinensis* (Plant)	[31]

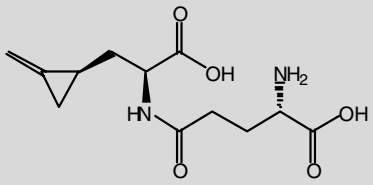 Hypoglycin B ($C_{12}H_{18}N_2O_5$)	m.w.: 270.2 HBD: 5 HBA: 7 C log P: -1.6 Violations: 0	*Blighia sapida* (Plant)	[32]
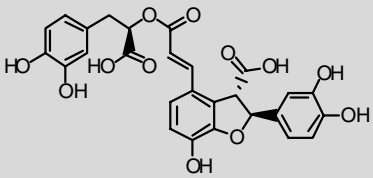 Lithospermic acid ($C_{27}H_{22}O_{12}$)	m.w.: 538.4 HBD: 7 HBA: 12 C log P: 1.34 Violations: 3	*Salvia mitiorrhiza* (Plant)	[33]
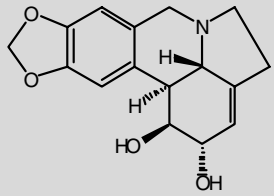 Lycorine ($C_{16}H_{17}NO_4$)	m.w.: 287.3 HBD: 2 HBA: 5 C log P: 0.39 Violations: 0	*Clivia miniata* (Plant)	[34]
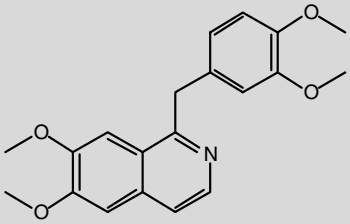 Papaverine ($C_{20}H_{21}NO_4$)	m.w.: 339.3 HBD: 0 HBA: 5 C log P: 3.7 Violations: 0	*Papaver somniferum* (Plant)	[35]
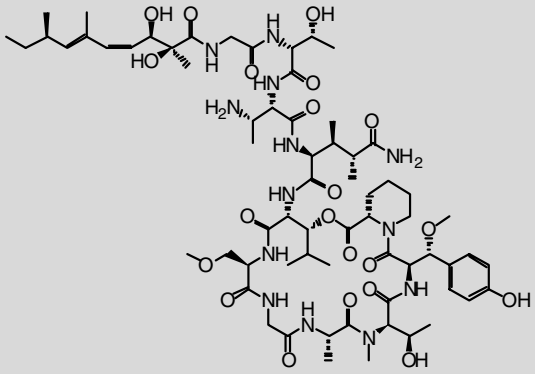 Papuamide A ($C_{66}H_{105}N_{13}O_{21}$)	m.w.: 1416 HBD: 18 HBA: 34 C log P: 1.3 Violations: 3	*Theonella swinhoe* (Marine sponge)	[36]
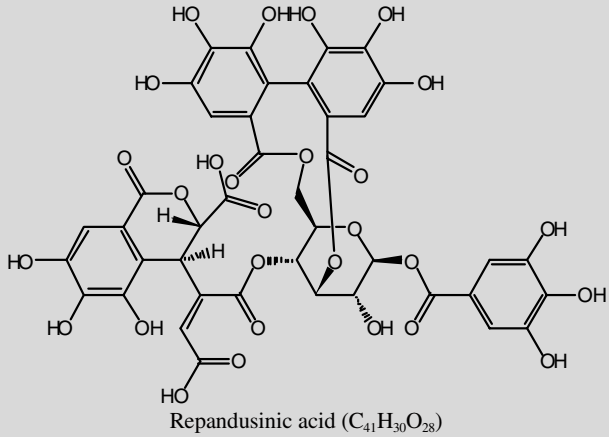 Repandusinic acid ($C_{41}H_{30}O_{28}$)	m.w.: 970.6 HBD: 15 HBA: 28 C log P: -0.2 Violations: 3	*Phyllanthus niruri* (Plant)	[37]

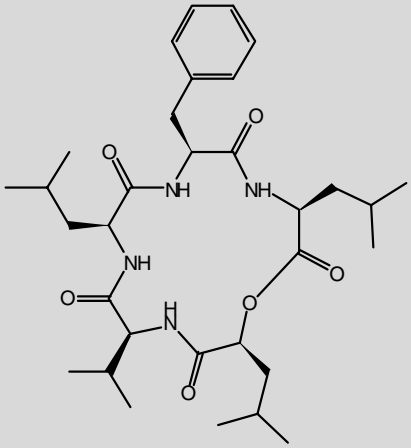 Sansalvamide A ($C_{32}H_{50}N_4O_6$)	m.w.: 586.7 HBD: 4 HBA: 10 C log P: 7.1 Violations: 1	*Fusarium sp* (Marine fungi)	[38]
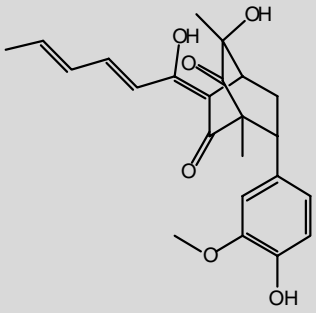 Sorbicatechol A ($C_{23}H_{26}O_6$)	m.w.: 398.4 HBD: 3 HBA: 6 C log P: 2.3 Violations: 0	*Penicillium chrysogenum* PJX-17 (Marine fungus)	[39]
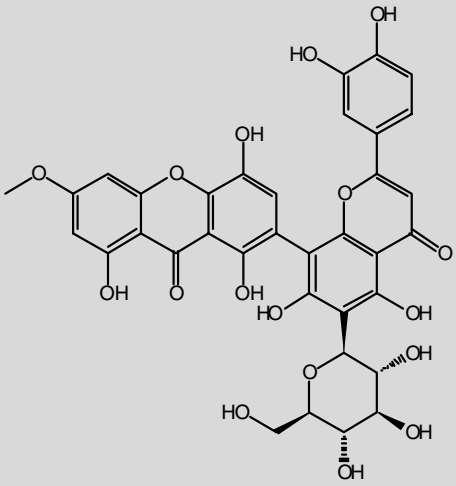 Swertifrancheside ($C_{35}H_{28}O_{17}$)	m.w.: 720.5 HBD: 11 HBA: 17 C log P: 2.6 Violations: 3	*Fagopyram esculentum* (Plant)	[40]
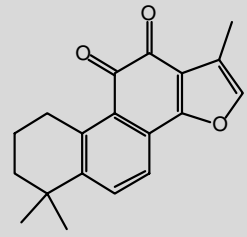 Tanshinone II A ($C_{19}H_{18}O_3$)	m.w.: 294.3 HBD: 0 HBA: 3 C log P: 5.7 Violations: 1	*Salvia miltiorrhiza* (Plant)	[41]

where HBD-Hydrogen bond donor, HBA-Hydrogen bond acceptor

flavonoids, lignans, coumarin, glycosides, peptide and amino acid used in this study were reported to have significant antiviral activity. To ensure the interaction between the selected natural compounds and corona-SARS 2 disease associated target COVID-19 M^{pro}, the Autodock 4.2 tool was performed for molecular docking analysis. The results in Table-2 depicted the compound codes, binding energies, inhibition constants, number of hydrogen bonds and interacted amino acid residues. The outcome revealed that the top ten best interactions were found in the compounds halitulin (-8.41 Kcal/mol), baicalin (-7.78 Kcal/mol), valonolide (-7.34 Kcal/mol), 1,5-dicaffeoylquinic acid (-7.21 Kcal/mol), papaverine (-6.55 Kcal/mol),

TABLE-2
BINDING ENERGIES, INHIBITION CONSTANT, AND HYDROGEN BOND INTERACTION OF SELECTED NATURAL COMPOUNDS AGAINST COVID-19 M^{pro}

Compound name	Binding energy (Kcal/mol)	Inhibition constant	No. of hydrogen bonds	Interacted amino acid residues
1,5-Dicaffeoylquinic acid	-7.21	5.17 µM	8	Pro168 (2.52Å), Glu166 (3.39Å), His163 (3.26Å), His164 (2.42Å), Cys145 (2.84Å), Asn142 (2.51Å), Asn142 (2.38Å), Met165 (3.35Å)
22-O-(N-Me-L-valyl)-21-epiaflaquinolone B	19.85	–	–	–
Arisugacin A	-3.19	4.57 mM	7	Glu166 (2.49Å), His164 (3.06Å), Cys145 (2.67Å), Cys145 (2.87Å), Thr26 (3.19Å), Thr26 (3.07Å), Gly143 (3.38Å)
Azadirachtin	3740	–	–	–
Baicalin	-7.78	1.99 µM	7	Met165 (3.56Å), Cys145 (3.40Å), Glu166 (2.76Å), Asn142 (2.50Å), Leu141 (3.04Å), Glu166(2.86Å), Phe140(2.52Å)
Berberine	-6.49	17.59 µM	6	Glu166 (2.99Å), Glu166 (4.09Å), Glu166 (3.86Å), His164 (3.21Å), His41 (3.21Å), His41 (3.52Å)
Butulinic acid	-5.75	60.68 µM	7	Lys5 (3.06Å), Gln127 (3.10Å), Gln127 (2.40Å), Gln127 (3.08Å), Lys137 (2.55Å), Gly138 (2.70Å), Ser139 (3.17Å)
Calonolide	-7.34	4.14 µM	6	Lys5 (3.34Å), Glu290 (2.82Å), Lys137 (2.87Å), Lys137 (3.35Å), Lys135 (3.35Å), Lys137 (3.04Å)
Conocurvone	11700	–	–	–
Cryptotanshinone	-6.29	24.71 µM	4	Leu141 (3.34Å), Phe140 (2.63Å), Phe140 (2.63Å), Glu166 (3.01Å)
Didemnin	11900	–	–	–
Gomisin A	-5.51	91.38 µM	6	Tyr126 (3.19Å), Ser139 (3.41Å), Lys137 (3.00Å), Gln127 (2.77Å), Lys5(4.22Å), Glu288 (2.80Å)
Halitulin	-8.41	680.6 nM	3	Val171 (3.41Å), Cys128 (3.67Å), Arg131 (3.20Å)
Hesperidin	-6.38	21.19 µM	8	Phe140 (2.71Å), Phe140 (3.39Å), LYS137 (2.92Å), LYS137 (3.39Å), Gly290 (3.00Å), Gly127 (3.26Å), Lys5 (2.75Å), Lys5 (3.05Å)
Hypoglycin B	-5.17	161.7 µM	7	Lys5 (2.55Å), Gln290 (2.56Å), Cys128 (3.26Å), Gln127 (2.62Å), Gln127 (3.11Å), Gln127 (2.51Å), Cys128 (3.2Å)
Lithosperimic acid	510.29	–	–	–
Lycorine	289.16	–	–	–
Papaverine	-6.55	15.93 µM	7	Lys5 (2.94Å), Ala7 (3.34Å), Ala7 (3.38Å), Gln12 7(3.30Å), Tyr126 (3.22Å), Gln127 (2.96Å), Gln290 (2.92Å)
Papuamide A	285000	–	–	–
Repandusinic acid	432.02	–	–	–
Sansalvamide A	-5.27	136.28 µM	6	Gly138 (3.18Å), Gly127 (3.08Å), Gln127 (2.96Å), Gln127 (3.22Å), Glu290 (3.14Å), Glu290 (2.57Å)
Sorbicatechol A	-5.41	108.27 µM	6	Val125 (3.28Å), Gln127 (3.13Å), Lys5 (3.36Å), Gln127 (2.73Å), Glu290 (2.79Å)
Swertifrancheside	60.49	–	–	–
Tanshinone II A	-6.1	33.88 µM	7	Asp289 (3.10Å), Glu288 (2.61Å), Lys5 (3.05Å), Lys5 (2.53Å), Gln127 (3.30Å), Tyr126 (3.54Å), Ser139 (3.57Å)

berberine (-6.49 Kcal/mol), hesperidin (-6.38 Kcal/mol), cryptotanshi-none (-6.29 Kcal/mol), tnshinone II A (-6.1 Kcal/mol) and butulinic acid (-5.75 Kcal/mol). Low affinity with the 6YB7-active site were found for gomisin A (-5.51 Kcal/mol), sansalv-amide A (-5.27 Kcal/mol), sorbicatechol A (-5.41 Kcal/mol), hypoglycin B (-5.17 Kcal/mol), arisugacin A (-3.19 Kcal/mol). The docking results further indicated that remaining 9 out of 24 of these compounds exhibited poor or no binding affinities since resulting all binding energies are positive values.

The negative sign in the free energy values shows the possibility of a spontaneous interaction between ligand and target receptor [42]. Based on molecular docking simulation results, the selected natural products that has lower free binding energy is halituline (-8.41 Kcal/mol). This result showed the strongest bond on COVID-19 M^{pro} than other compounds. halituline had an inhibition constant of 680.6 nM on COVID-19 M^{pro}. Inhibition constant shows the concentration that is required by the ligand in inhibiting macromolecules. The smaller the value of inhibition constant (Ki) is the better results due to the small concentration of ligand was required to inhibit the spread of newly identified corona virus. The compounds remaining top ten baicalin, calonolide,1,5-dicaffeoylquinic acid, papaverine, berberine, cryptotanshinone, tnshinone II A and butulinic acid showed varied binding energy ranging -7.78 to -5.75 Kcal/mol. The weakest binding energy (-3.19 Kcal/mol) was shown by arisugacin A whereas halituline showed the strongest binding energy (-8.41 Kcal/mol). They also showed lower inhibition constant ranging 161.78 to 1.99 µM compared to those of other compounds.

The nature of the intermolecular interaction formed with amino acid residue of COVID-19 M^{pro} were investigated for the docking scored compounds. The docking poses of selected natural products with negative binding free energy are shown in Fig. 2. A closer look at the interaction between compound halituline and COVID-19 M^{pro} revealed that the functional

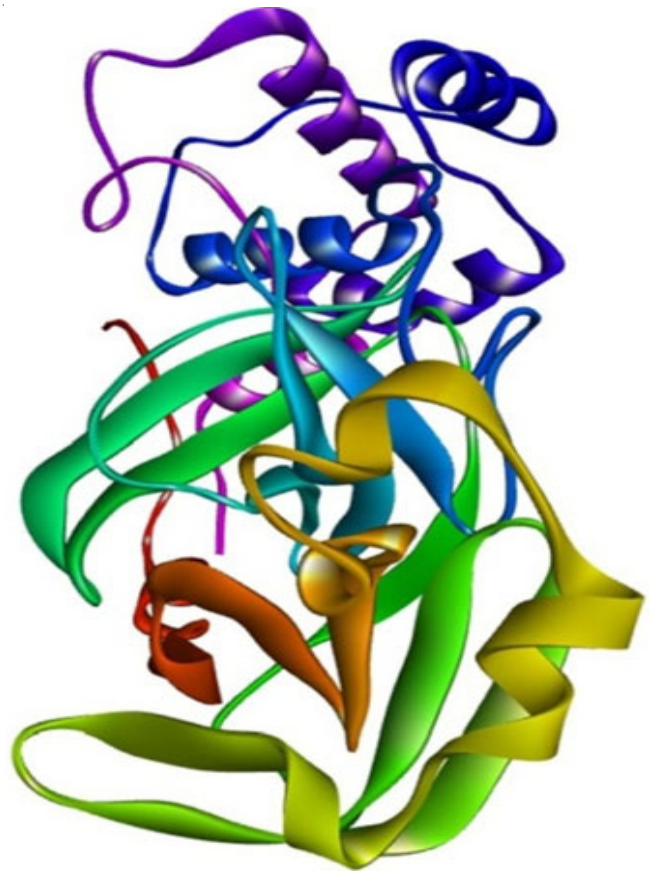

Fig 1. COVID-19 M^{pro} (PDB ID: 6YB7) in discovery studio visualizer

group in halituline bound *via* three strong hydrogen bond to residue Val171, Cys128, Arg131, which are present in COVID-19 M^{pro}. The second scored compound baicalin showed seven H-bond interaction with COVID-19 M^{pro} residues Met165, Cys 145, Glu166, Asn142, Leu141, Glu166 and Phe140. The remaining all other selected compounds with good binding affinity *via* hydrogen bond interactions with COVID-19 M^{pro} residues are listed in Table-2.

It is interesting to note that among the top 10 inhibitors, the most promising inhibitors of the SARS-CoV-2 M^{pro} (Table-2) are primarily represented by a class of molecules called alkaloids (halitulin, papaverine and berberine), terpenoids (cryptotanshinone, tanshinone II A and butulinic acid) and glycosides (baicalin and hesperidin). The alkaloid halitulin showed lesser binding energy (-8.41 Kcal/mol) among the all the docked compounds, which suggest high affinity to the receptor. Moreover, the drug-like predictions showed that most of the screened natural compounds followed the Lipinski′s rule of five. Molecular docking and pharmacokinetics studies showed that most of compounds fulfill the requirement for binding the active sites of COVID-19 M^{pro}, such as binding affinity, inhibition constant and hydrogen bonds (Fig. 2). Therefore, it is suggested that for future *in vitro* and *in vivo* studies and possible clinical trials.

Conclusion

In present study, a computational approach is accessed to predict inhibitors for COVID-19 M^{pro} by exploring docking of 24 natural compounds with COVID-19 M^{pro} protein. Base

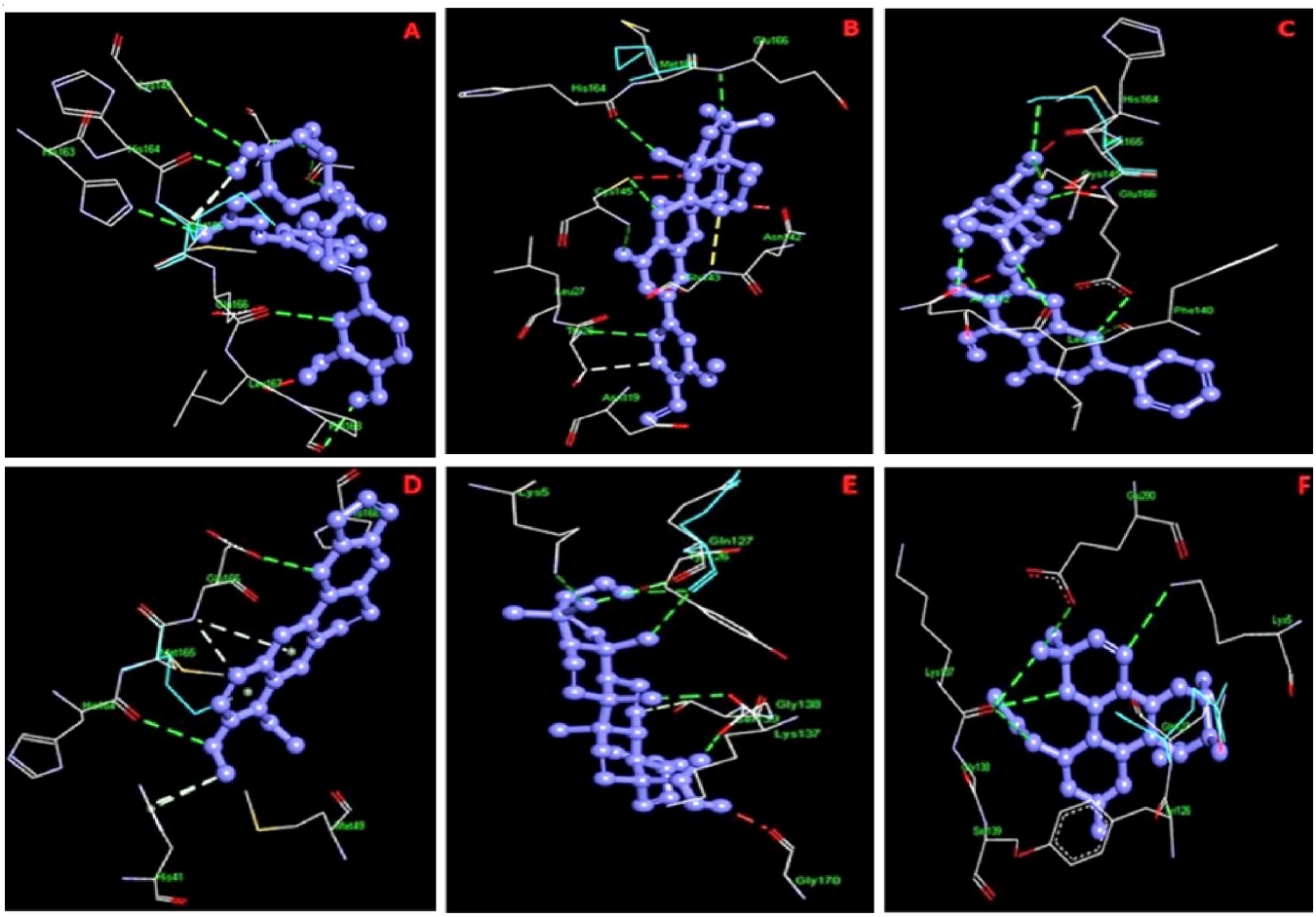

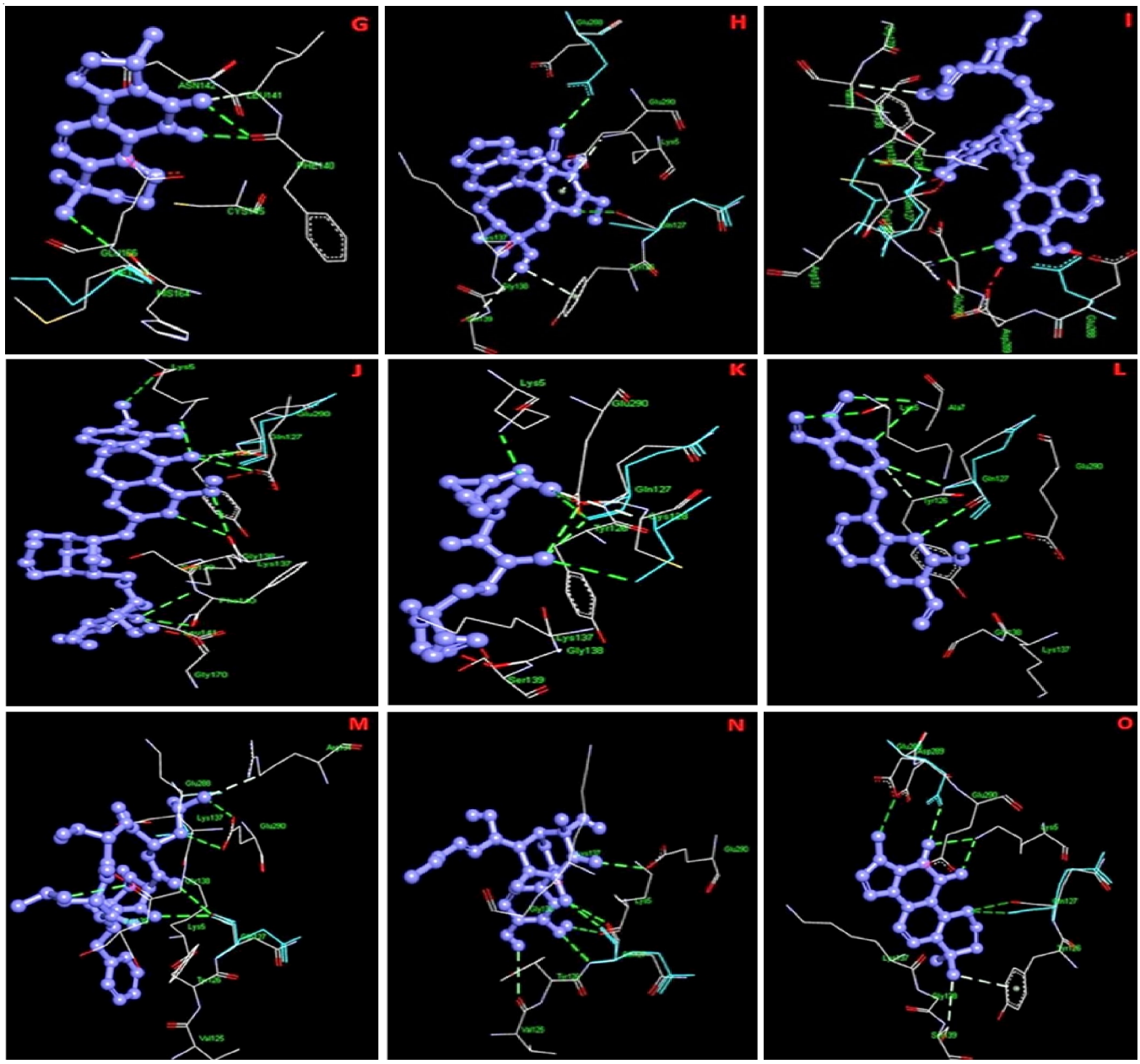

Fig 2. Docking pose of selected antiviral natural products are shown with the binding pocket residues and interacting residues with COVID-19 M^{pro} (PDB ID:6YB7). (A) 1,5-dicaffeoylquinic acid, (B) Arisugacin A, (C) Baicalin, (D) Berberine, (E) Butulinic acid, (F) Calonolide, (G) Cryptotanshinone, (H) Gomisin A, (I) Halitulin, (J) Hesperidin, (K) Hypoglycin B, (L) Papaverine (M), Sansalvamide A, (N) Sorbicatechol A and (O) Tanshinone II A

on the molecular docking studies the natural compounds halitulin, baicalin, calonolide, 1,5-dicaffeoylquinic acid, papaverine, berberine, hesperidin, cryptotanshinone, tnshinone II A and butulinic acid can serve as source of SARS-CoV-2 drugs and showed a better binding energy score for COVID-19 target. Future *in vitro* activity assay of the ligands identified in this study will give vital information on new scaffolds for lead optimization.

REFERENCES

1. L. van der Hoek, Human coronaviruses: What do They Cause?, *Antivir. Ther.*, **12**, 651 (2007).
2. C. Geller, M. Varbanov and R.E. Duval, Human Coronaviruses: Insights into Environmental Resistance and Its Influence on the Development of New Antiseptic Strategies, *Viruses*, **4**, 3044 (2012); https://doi.org/10.3390/v4113044
3. P. Mukherjee, P. Desai, L. Ross, E.L. White and M.A. Avery, Structure-Based Virtual Screening Against SARS-3CL^{pro} to Identify Novel Non-peptidic Hits, *Bioorg. Med. Chem.*, **16**, 4138 (2008); https://doi.org/10.1016/j.bmc.2008.01.011
4. L.L. Chen, J. Li, C. Luo, H. Liu, W.J. Xu, G. Chen, O.W. Liew, W.L. Zhu, C.M. Puah, X. Shen and H.L. Jiang, Binding Interaction of Quercetin-3-β-galactoside and Its Synthetic Derivatives with SARS-CoV 3CL^{pro}: Structure-Activity Relationship Studies Reveal Salient Pharmacophore Features, *Bioorg. Med. Chem.*, **14**, 8295 (2006); https://doi.org/10.1016/j.bmc.2006.09.014
5. J.F. Chan, K.S. Li, K.K. To, V.C. Cheng, H. Chen and K.Y. Yuen, Is the Discovery of the Novel Human Betacoronavirus 2c EMC/2012 (HCoV-EMC) the Beginning of Another SARS-Like Pandemic, *J. Infect.*, **65**, 477 (2012); https://doi.org/10.1016/j.jinf.2012.10.002
6. D. Paraskevis, E.G. Kostaki, G. Magiorkinis, G. Panayiotakopoulos, G. Sourvinos and S. Tsiodras, Full-Genome Evolutionary Analysis of the

Novel Coronavirus (2019-nCoV) Rejects the Hypothesis of Emergence as a Result of a Recent Recombination Event, *Infect. Genet. Evol.*, **79**, 104212 (2020); https://doi.org/10.1016/j.meegid.2020.104212
7. https://www.who.int/emergencies/diseases/novel-coronavirus-2019/situation-reports
8. P. Ruwali, N. Rai, N. Kumar and P. Goutam, Antiviral Potential of Medicinal Plants: An Overview, *Int. Res. J. Pharm.*, **4**, 8 (2013); https://doi.org/10.7897/2230-8407.04603
9. C.D. Owen, P. Lukacik, C.M. Strain-Damerell, A. Douangamath, A.J. Powell, D. Fearon, J. Brandao-Neto, A.D. Crawshaw, D. Aragao, M. Williams, R. Flaig, D. Hall, K. McAauley, D.I. Stuart, F. Von Delft and M.A. Walsh, COVID-19 Main Protease with Unliganded Active Site (2020).
10. S.M.D. Rizvi, S. Shakil and M. Haneef, A Simple Click by Click Protocol to Perform Docking: AutoDock 4.2 Made Easy for Non-Bioinformaticians, *Excli J.*, **12**, 831 (2013).
11. C.A. Lipinski, F. Lombardo, B.W. Dominy and P.J. Feeney, Experimental and Computational Approaches to Estimate Solubility and Permeability in Drug Discovery and Development Settings, *Adv. Drug Deliv. Rev.*, **64**, 4 (2012); https://doi.org/10.1016/j.addr.2012.09.019
12. T. Ganyani, C. Kremer, D. Chen, A. Torneri, C. Faes and J. Wallinga, Estimating the Generation Interval for COVID-19 based on Symptom Onset Data, *medRxiv Preprint* (2020); https://doi.org/10.1101/2020.03.05.20031815
13. B. Liu and J. Zhou, SARS-CoV Protease Inhibitors Design using Virtual Screening Method from Natural Products Libraries, *J. Comput. Chem.*, **26**, 484 (2005); https://doi.org/10.1002/jcc.20186
14. N. Ansari and F. Khodagholi, Natural Products as Promising Drug Candidates for the Treatment of Alzheimer's Disease: Molecular Mechanism Aspect, *Curr. Neuropharmacol.*, **11**, 414 (2013); https://doi.org/10.2174/1570159X11311040005
15. H. Kubinyi, Drug Research: Myths, Hype and Reality, *Nat. Rev. Drug Discov.*, **2**, 665 (2003); https://doi.org/10.1038/nrd1156
16. P. Srinivasan, S. Vijayakumar, S. Kothandaraman and M. Palani, Anti-Diabetic Activity of Quercetin Extracted from *Phyllanthus emblica* L. Fruit: *in silico* and *in vivo* Approaches, *J. Pharm. Anal.*, **8**, 109 (2018); https://doi.org/10.1016/j.jpha.2017.10.005
17. Y. Li, P.P. But and V.E. Ooi, ANtiviral Activity and Mode of Action of Caffeoylquinic Acids from *Schefflera heptaphylla* (L.) Frodin, *Antiviral Res.*, **68**, 1 (2005); https://doi.org/10.1016/j.antiviral.2005.06.004
18. C. Prieto and J.M. Castro, Porcine Reproductive and Respiratory Syndrome Virus Infection in the Boar: A Review, *Theriogenology*, **63**, 1 (2005); https://doi.org/10.1016/j.theriogenology.2004.03.018
19. X.H. Nong, Y.F. Wang, X.Y. Zhang, M.P. Zhou, X.Y. Xu and S.H. Qi, Territrem and Butyrolactone Derivatives from a Marine-Derived Fungus Aspergillus Terreus, *Mar. Drugs*, **12**, 6113 (2014); https://doi.org/10.3390/md12126113
20. M.M. Parida, C. Upadhyay, G. Pandya and A.M. Jana, Inhibitory potential of Neem (*Azadirachta indica* Juss) Leaves on Dengue virus Type-2 Replication, *J. Ethnopharmacol.*, **79**, 273 (2002); https://doi.org/10.1016/S0378-8741(01)00395-6
21. Z. Keivan, T.T. Boon, S.S. Teoh, F.W. Pooi and A. Sazaly, P02.158. Tai Chi Community Program is Effective in Reducing Elderly Fall-Related Hospital Utilization: A Prospective Observational Study, *BMC Complement. Altern. Med.*, **12**, 214 (2012); https://doi.org/10.1186/1472-6882-12-S1-P214
22. K. Hayashi, K. Minoda, Y. Nagaoka, T. Hayashi and S. Uesato, Antiviral Activity of Berberine and Related Compounds against Human Cytomegalovirus, *Bioorg. Med. Chem. Lett.*, **17**, 1562 (2007); https://doi.org/10.1016/j.bmcl.2006.12.085
23. N.I. Pavlova, O.V. Savinova, S.N. Nikolaeva, E.I. Boreko and O.B. Flekhter, Antiviral Activity of Betulin, Betulinic and Betulonic Acids Against Some Enveloped and Non-enveloped Viruses, *Fitoterapia*, **74**, 489 (2003); https://doi.org/10.1016/S0367-326X(03)00123-0
24. M.J. Currens, R.J. Gulakowski, J.M. Mariner, R.A. Moran, R.W. Buckheit, K.R. Gustafson, J.B. McMahon and M.R. Boyd, Antiviral Activity and Mechanism of Action of Calanolide A against the Human Immunodeficiency Virus Type-1, *J. Pharmacol. Exp. Ther.*, **279**, 645 (1996).
25. J.H. Peter, Compounds with Anti-HIV Activity from Plants, *Trans. Royal Soc. Trop. Med. Hyg.*, **90**, 604 (1996); https://doi.org/10.1016/S0035-9203(96)90403-4
26. B.-Q. Wang, *Salvia miltiorrhiza*: Chemical and Pharmacological Review of a Medicinal Plant, *J. Med. Plants Res.*, **4**, 2813 (2010).
27. P.G. Canonico, W.L. Pannier, J.W. Huggins and K.L. Rienehart, Inhibition of RNA Viruses *in vitro* and in Rift Valley Fever-Infected Mice by Didemnins A and B, *Antimicrob. Agents Chemother.*, **22**, 696 (1982); https://doi.org/10.1128/AAC.22.4.696
28. K. Yasukawa, Y. Ikeya, H. Mitsuhashi, M. Iwasaki, M. Aburada, S. Nakagawa, N. Takeuchi and M. Takido, Gomisin A Inhibits Tumor Promotion by 12-O-Tetra-decanoylphorbol-13-Acetate in Two-Stage Carcinogenesis in Mouse Skin, *Oncology*, **49**, 68 (1992); https://doi.org/10.1159/000227014
29. A.C. da Silva, J.M. Kratz, F.M. Farias, A.T. Henriques, J. dos Santos, R.M. Leonel, C. Lerner, B. Mothes, C.R.M. Barardi and C.M.O. Simões, *In Vitro* Antiviral Activity of Marine Sponges Collected Off Brazilian Coast, *Biol. Pharm. Bull.*, **29**, 135 (2006); https://doi.org/10.1248/bpb.29.135
30. G. Poonam, Chemical Constituents of *Haliclona*: An Overview, *J. Pharmacogn. Phytochem.*, **8**, 823 (2019).
31. A. Paredes, M. Alzuru, J. Mendez and M. Rodríguez-Ortega, Anti-Sindbis Activity of Flavanones Hesperetin and Naringenin, *Biol. Pharm. Bull.*, **26**, 108 (2003); https://doi.org/10.1248/bpb.26.108
32. X. Xu, H. Xie, Y. Wang and X. Wei, A-Type Proanthocyanidins from Lychee Seeds and Their Antioxidant and Antiviral Activities, *J. Agric. Food Chem.*, **58**, 11667 (2010); https://doi.org/10.1021/jf1033202
33. I.S. Abd-Elazem, H.S. Chen, R.B. Bates and R.C. Huang, Isolation of Two Highly Potent and Non-toxic Inhibitors of Human Immunodeficiency Virus Type 1 (HIV-1) Integrase from *Salvia miltiorrhiza*, *Antiviral Res.*, **55**, 91 (2002); https://doi.org/10.1016/S0166-3542(02)00011-6
34. P.L. Wang, L.F. Li, Q.Y. Wang, L.Q. Shang, P.Y. Shi and Z. Yin, Anti-Dengue-Virus Activity and Structure-Activity Relationship Studies of Lycorine Derivatives, *ChemMedChem*, **9**, 1522 (2014); https://doi.org/10.1002/cmdc.201300505
35. M. Aggarwal, G.P. Leser and R.A. Lamb, Repurposing Papaverine as an Antiviral Agent against Influenza Viruses and Paramyxoviruses, *J. Virol.*, **94**, 19 (2020); https://doi.org/10.1128/JVI.01888-19
36. C.D. Andjelic, V. Planelles and L.R. Barrows, Characterizing the Anti-HIV Activity of Papuamide A, *Mar. Drugs*, **6**, 528 (2008); https://doi.org/10.3390/md20080027
37. A.D. Naik and A.R. Juvekar, Effects of Alkaloidal Extract of *Phyllanthus niruri* on HIV Replication, *Indian J. Med. Sci.*, **57**, 387 (2003).
38. Y. Hwang, D. Rowley, D. Rhodes, J. Gertsch, W. Fenical and F. Bushman, Mechanism of Inhibition of a Poxvirus Topoisomerase by the Marine Natural Product Sansalvamide A, *Mol. Pharmacol.*, **55**, 1049 (1999); https://doi.org/10.1124/mol.55.6.1049
39. S.Z. Moghadamtousi, S. Nikzad, H.A. Kadir, S. Abubakar and K. Zandi, Potential Antiviral Agents from Marine Fungi: An Overview, *Mar. Drugs*, **13**, 4520 (2015); https://doi.org/10.3390/md13074520
40. J.-N. Wang, C.-Y. Hou, Y.-L. Liu, L.-Z. Lin, R.R. Gil and G.A. Cordell, Swertifrancheside, An HIV-Reverse Transcriptase Inhibitor and the First Flavone-Xanthone Dimer, from *Swertia franchetiana*, *J. Nat. Prod.*, **57**, 211 (1994); https://doi.org/10.1021/np50104a003
41. N. Sun, P. Sun, M. Yao, A. Khan, Y. Sun, K. Fan, W. Yin and H. Li, Autophagy Involved in Antiviral Activity of Sodium Tanshinone IIA Sulfonate against Porcine Reproductive and Respiratory Syndrome Virus Infection *in vitro*, *Antivir. Ther.*, **24**, 27 (2018); https://doi.org/10.3851/IMP3268
42. G.M. Morris, D.S. Goodsell, R.S. Halliday, R. Huey, W.E. Hart, R.K. Belew and A.J. Olson, Automated Docking Using a Lamarckian Genetic Algorithm and An Empirical Binding Free Energy Function, *J. Comput. Chem.*, **19**, 1639 (1998); https://doi.org/10.1002/(SICI)1096-987X(19981115)19:14<1639::AID-JCC10>3.0.CO;2-B